

Simultaneous Determination of Acetaminophen and Tyrosine Using Screen-printed Electrochemical Sensor Based on MWCNTs-doped Poly(glycine)/Poly(acrylic acid) Conducting Polymers

Zhiqiang Wei¹, Shaofang Guo², Liuyang Cheng¹, Ting Li¹, Yanli Zhang¹, Hui Yang^{1,*}

¹ College of Medical, Henan University of Science and Technology, Luoyang, 471023, China.

² Hospital of Henan University of Science and Technology, Luoyang, 471023, China.

*E-mail: yanghui7761@163.com

Received: 5 February 2019 / Accepted: 26 April 2019 / Published: 10 June 2019

A sensitive electrochemical sensor for the simultaneous determination of acetaminophen (ACOP) and tyrosine (Tyr) was proposed based on MWCNTs-doped poly (glycine) (p-gly)/ poly (acrylic acid) (PAA) conducting polymers modified screen-printed electrode (SPE). The incorporation of MWCNTs and p-gly/ PAA composite conductive polymers brought about enhanced electro-catalytic activity and additional binding sites for ACOP and Tyr. Cyclic voltammetry (CV) and linear sweep voltammetry (LSV) were performed to investigate the electrochemical behaviors of ACOP and Tyr. Under the optimal experimental conditions, the oxidation peak currents of ACOP and Tyr increased linearly with two concentration intervals over the range of 0.25-120 μM and 0.4-150 μM , respectively. The detection limits ($S/N = 3$) were 0.08 μM for ACOP and 0.13 μM for Tyr. Moreover, the sensor has been successfully applied for the determination of ACOP and Tyr in human serum samples, showing its great application prospects in pharmaceutical analysis.

Keywords: Screen-printed Electrode, Poly (glycine), Poly (acrylic acid), Acetaminophen, Tyrosine

1. INTRODUCTION

Acetaminophen (N-(4-hydroxyphenyl) acetamide, ACOP) is commonly used as a safe and effective pain killer for head ache, backache, arthritis and postoperative pain, and it can also be used to relieve cough, cold, and fevers symptoms [1-2]. It has low toxicity when used at the recommended doses. However, overdoses of ACOP induce the accumulation of toxic metabolites, which may cause liver and kidney damage, and possibly mortality [3]. Tyrosine (4-hydroxyphenylalanine, Tyr) is an essential aromatic amino acid and vital constituent of proteins, which is indispensable in human nutrition for establishing and maintaining a positive nitrogen balance [4-5]. Tyr exists in dairy products, eggs, beans

and meats, and it has a vital role in production of several important neurotransmitters in brain that help nerve cell communicate. The absence of Tyr can lead to albinism, hypochondria, or depression [6-7]. In contrast, high Tyr concentration increases sister chromatid exchange [8].

It was found that ACOP alter the concentration level of serotonin by producing peroxynitrite (ONOO⁻), which reacts with tyrosine to form (2S)-2-amino-3-(4-hydroxy-3-nitrophenyl) propanoic acid [9-10]. This product at the micromolar level may cause vascular endothelial dysfunction through promotion of DNA damage and/or apoptosis and also cause neurodegeneration [9-10]. Therefore, it is very important to develop an analytical technique for simultaneous determination of ACOP and Tyr in pharmaceutical dosages and human fluids.

In recent years, various analytical methods, such as UV/Vis spectrophotometry [11], HPLC [12], chemiluminescence [13], capillary electrophoresis [14] and electrochemical methods [15-17] have been reported for the determination of ACOP or Tyr. Among them, electrochemical detection are ideal methods for directly and selectively getting information from a complex system, because of its advantages of simple, rapid, sensitive and cost effective. Nevertheless, improving the analytical method in terms of sensitivity, stability, repeatability and selectivity are still essential for human health and security [2,18].

Nanomaterial-doped conducting polymers represent a unique class of composite materials that synergizes the advantageous features of nanomaterials and organic conductors. So, they have been used in many applications such as electrochemical sensors and energy storage devices [19]. Because of the unique structures and properties of MWCNTs, such as good electrical conductivity, high electrocatalytic effect, strong adsorptive ability and low price, MWCNTs have been widely used for developing highly sensitive chemical modified electrodes [20]. Conducting polymers can be controllably synthesized from various monomers, and during the polymerization process, different nanomaterials offering unique physical and chemical properties can be doped into the formed conducting polymer composites [19]. Poly (acrylic acid) (PAA) is a weak polyelectrolyte that has wide industrial applications [21]. Glycine (2-aminoacetic acid, gly) has a strong hydrophilic property, and can be immobilized on the modified electrode surface by electrochemical polymerization [22]. MWCNTs, as dopants, can bring the p-gly/PAA conducting polymer enhanced or even new properties, such as large surface area, enhanced conductivity and strength, and additional functional groups.

Herein, we explored the simultaneous determination of ACOP and Tyr using MWCNTs-doped p-gly/PAA conducting polymer modified screen-printed electrode (p-gly/PAA/MWCNTs/SPE). The p-gly/PAA/MWCNTs/SPE is found to exhibit greater electrocatalytic activity, stability, and reproducibility for the simultaneous determination of ACOP and Tyr in Britton-Robinson buffer solution (BRBS) than unmodified/bare SPE. Furthermore, the proposed p-gly/PAA/MWCNTs/SPE electrochemical sensor was employed to detect ACOP and Tyr in human serum samples.

2. EXPERIMENT

2.1 Reagents and apparatus

All reagents were analytical grade and had not been further purified. ACOP, Tyr, PAA and glycine were purchased from Aladdin Reagent (Shanghai, China). Dipotassium hydrogen phosphate

(K_2HPO_4), potassium dihydrogen phosphate (KH_2PO_4), acetic acid (CH_3COOH), boric acid (H_3BO_3), phosphoric acid (H_3PO_4) and potassium ferricyanide ($K_3[Fe(CN)_6]$) were purchased from Tianjin Damao Chemical Reagent (Tianjin, China) and Sinopharm Chemical Reagent (Shanghai, China). All required solutions were prepared using ultrapure water (Millipore, USA).

Multi-walled carbon nanotubes (MWCNTs) (>97% purity, <2 μm length and 10-20 nm internal diameter) were purchased from Nanotech Port (Shenzhen, China). The MWCNTs were functionalized with carboxyl group according to literature [23]. Commercially available integrated three-electrode screen-printed electrode (SPE) (DropSens) with a carbon working electrode (4 mm diameter), a platinum auxiliary electrode and silver reference electrode was used to carry out the experiments.

Electrochemical measurements were performed on a CHI 830D electrochemical analyzer equipped with data processing software (Shanghai Chenhua Instrument Co., Ltd, Shanghai, China). The pH measurements were performed using a PHS-3C digital pH meter (INESA Scientific Instrument Co., Ltd, Shanghai, China).

2.2. Fabrication of p-gly/PAA /MWCNTs/SPEs

As illustrated in Fig. 1(A), firstly, bare SPE was placed horizontally on the table and a self-adhesive Polyethylene terephthalate (PET) label paper with a thickness of 12 μm was used to make a ring with an inner diameter of 4 mm and an outer diameter of 6 mm. The ring was pasted between carbon working electrode and silver reference electrode of the SPE. Subsequently, 3 mg MWCNTs was stacked on the carbon working electrode of the SPE, and 20 μL H_2O containing 0.1% PAA was added into the MWCNTs. Then the slurry containing MWCNTs and PAA was scraped flat with a cover slip, and the ring was removed immediately. After standing for 1 hour, the MWCNTs-doped PAA conducting polymers modified SPE (PAA/MWCNTs/SPE) was prepared. Finally, the PAA/MWCNTs/SPE was immersed in 0.1M phosphate buffered solution (pH 6.0) containing 15 μM glycine, and the MWCNTs-doped p-gly/PAA conducting polymers modified SPE (p-gly/PAA/MWCNTs/SPE) was obtained by electrochemical polymeric deposition with CV. The cyclic scans were executed by applying definite consecutive potential cycles at the potential range of -0.45 to +1.85 V (vs. Ag/AgCl), with initial potential of -0.45 V, 10 scan cycles and scan rate of 100 $mV \cdot s^{-1}$ [22]. The p-gly/PAA/MWCNTs/SPE was rinsed thoroughly with water after the electrochemical processing. Fig. 1 (B) illustrated the construction process of MWCNTs-doped p-gly/PAA conducting polymers electrochemical sensing interface and the basic principle of detecting ACOP and Tyr.

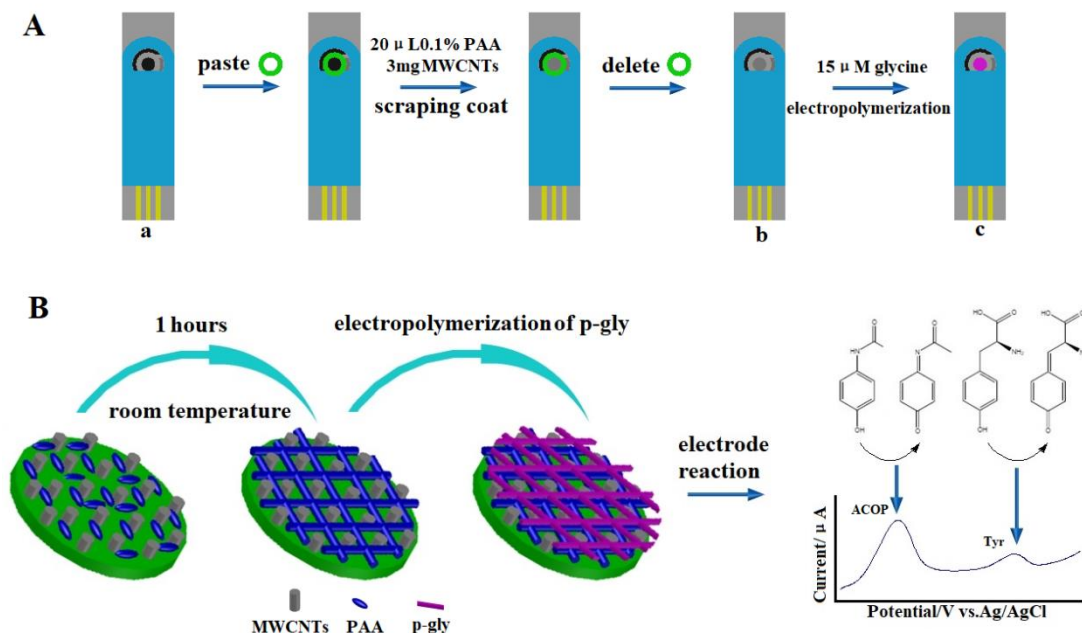


Figure 1. (A) Schematic illustrations of p-gly/PAA/MWCNTs/SPE fabrication (bare SPE (a), PAA/MWCNTs/SPE (b) and p-gly/PAA/MWCNTs/SPE (c)). (B) MWCNTs-doped p-gly/PAA conducting polymers electrochemical sensing interface.

2.3 Analysis of ACOP and Tyr in real samples

Fresh human blood was collected from healthy volunteers in Henan University of Science and Technology First Affiliated Hospital. The collected blood sample was kept at room temperature for 30 minutes and then centrifuged for 5 minutes at 3500 rpm. Finally, the supernatant serum was collected in a new test tube and stored at 4 °C in a refrigerator when not in use. 200 μL serum was transferred into the electrochemical cell and diluted to 10 mL with BRBS (pH 5.0). Different concentrations of ACOP and Tyr were added to electrochemical cell containing serum samples and BRBS (pH 5.0). Linear sweep voltammetry (LSV) was recorded with the potential range of 0.25 to 0.8 V (vs. Ag/AgCl) at scan rate of 50 mV·s⁻¹.

3. RESULTS and DISCUSSION

3.1. Electrochemical behavior of ACOP and Try on p-gly/PAA/MWCNTs/SPE

As shown in Fig. 2A, p-gly/PAA/MWCNTs/SPE showed an efficient electro-catalytic activity for the oxidation of ACOP and Tyr molecules compared to PAA/MWCNTs/SPE and bare SPE. In the cyclic voltammetric curves, two reversible redox peaks of ACOP were observed, but no reduction peak had been observed of Tyr. ACOP and Tyr exhibited well defined oxidation peaks around 0.25 and 0.55 V at p-gly/PAA/MWCNTs/SPE, respectively. The peak potentials difference of about 0.3 V between the two oxidation peaks of ACOP and Tyr. These indicated that the p-gly/PAA/MWCNTs/SPEs showed high sensitivity and good peak potential separation in the determination of ACOP and Tyr.

Fig. 2B showed the peak heights of 10 μM ACOP and 20 μM Tyr in BRBS with pH 6.0 in

different scan rates in the range of 10-70 $\text{mV}\cdot\text{s}^{-1}$. The analysis of peak height against the square root of scan rate was found to be linear (ACOP: $I_{\text{pa}}/\mu\text{A} = 66.49 (\text{V}\cdot\text{s}^{-1})^{1/2} - 4.49 \mu\text{A}$, $R^2 = 0.996$; Tyr: $I_{\text{pa}}/\mu\text{A} = 72.15 (\text{V}\cdot\text{s}^{-1})^{1/2} - 5.83 \mu\text{A}$, $R^2 = 0.994$), which suggested the diffusion controlled electrode processes [24].

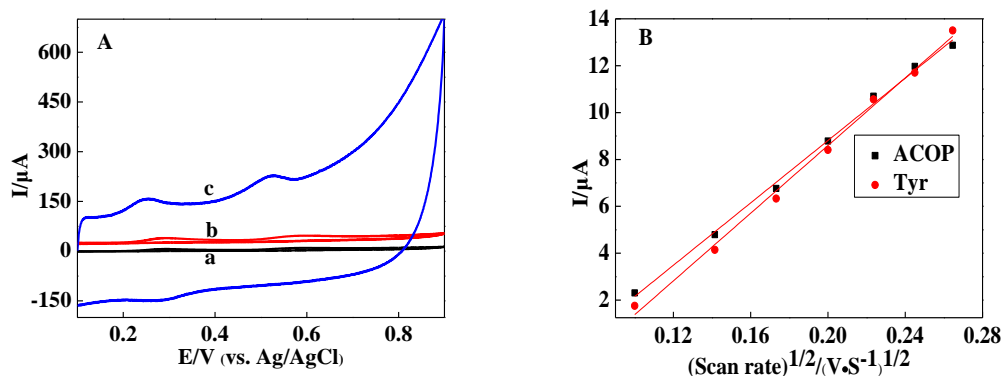


Figure 2. (A) Cyclic voltammetric curves of bare SPE (a), PAA/MWCNTs/SPE (b) and p-gly/PAA/MWCNTs/SPE (c) in BRBS (pH6.0) containing 10 μM of ACOP and 20 μM of Try. (B) Cyclic voltammetric peak current analysis of p-gly/PAA/MWCNTs/SPE at various scan rates.

As shown in Fig. 3, with the contents of ACOP and Tyr in BRBS (pH 6.0) added successively, the current signals increased obviously. And we can found that due to the same content of ACOP or Tyr in two adjacent tests, the oxidation peaks of ACOP or Tyr in two adjacent cyclic voltammetric curves were almost overlapped. So, the simultaneous determination of ACOP and Tyr is allowed without mutual interference.

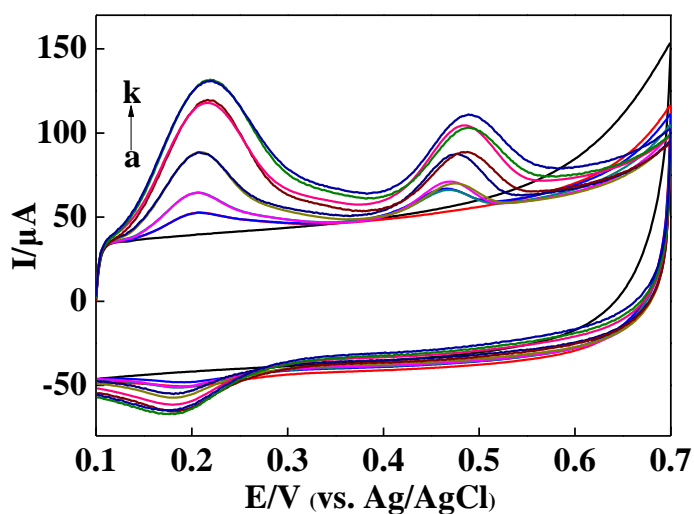


Figure 3. Cyclic voltammetric curves observed at p-gly/PAA/MWCNTs/SPE for successive additions of ACOP and Try into BRBS (pH 6.0) (a→k: bg, 10 μM of ACOP, 10 μM ACOP +20 μM Tyr, 20 μM ACOP +20 μM Tyr, 20 μM ACOP +30 μM Tyr, 50 μM ACOP +30 μM Tyr, 50 μM ACOP +70 μM Tyr, 100 μM ACOP +70 μM Tyr, 100 μM ACOP +100 μM Tyr, 120 μM ACOP +100 μM Tyr, 120 μM ACOP +120 μM Tyr. Scan rate: 50 $\text{mV}\cdot\text{s}^{-1}$).

3.2 Influence of detection buffer solution pH

Because the protons take part in the electrode reaction process of ACOP and Tyr, pH of the working buffer is very important for ACOP and Tyr detection. Thus, the current response and oxidation potential of ACOP and Tyr at p-gly/PAA/MWCNTs/SPE were investigated in BRBS with pH range from 2.0 to 6.0 by CV. The effect of pH was illustrated in Fig. 4A and Fig. 4B, peak currents of Tyr were amplified upon the decrease of buffer pH, and peak currents of ACOP didn't change much with the pH value. This result indicated that BRBS (pH 2.0) was the suitable supporting electrolyte solution for simultaneous determination of ACOP and Tyr. As shown in Fig. 4C, the relationships between the potentials and pH were linear (ACOP: $E_{pa} (V) = 0.6144 - 0.0668 \text{ pH}$, $R^2 = 0.993$; Tyr: $E_{pa} (V) = 0.8476 - 0.0615 \text{ pH}$, $R^2 = 0.997$). The slopes of the equations were close to the anticipated Nernstian value of -59 mV for electrochemical processes involving the same number of protons and electrons [24]. Therefore, we supposed that the oxidation of ACOP and Tyr at p-gly/PAA/MWCNTs/SPE is likely involves $2e^-/2H^+$ transfer processes as shown in Scheme 1.

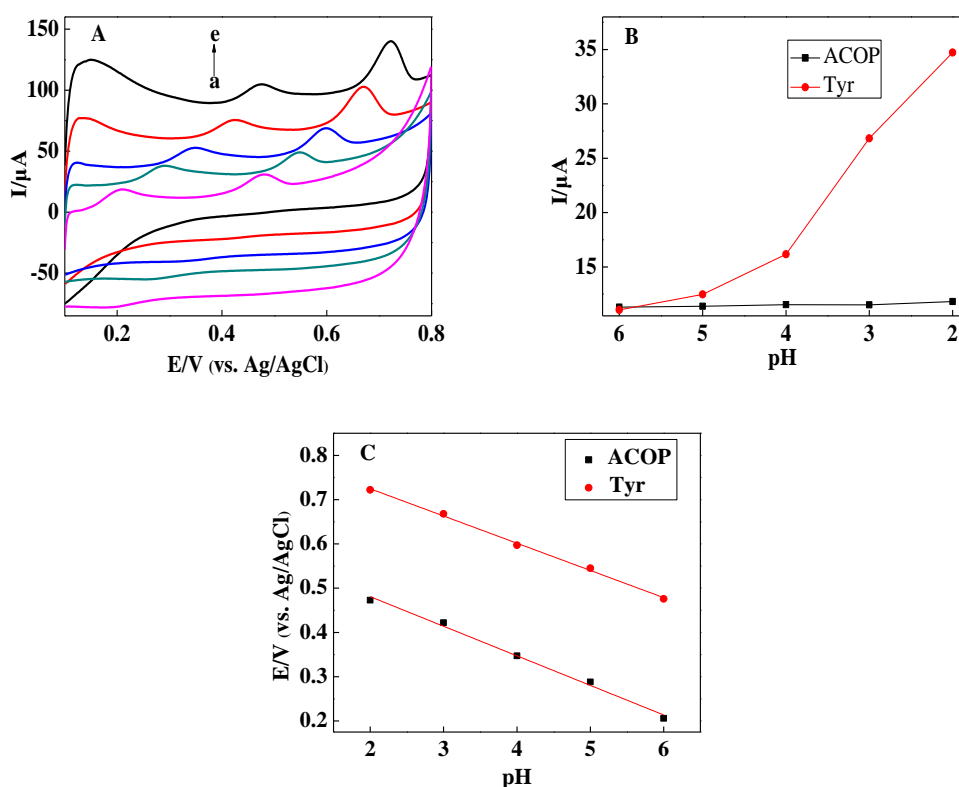
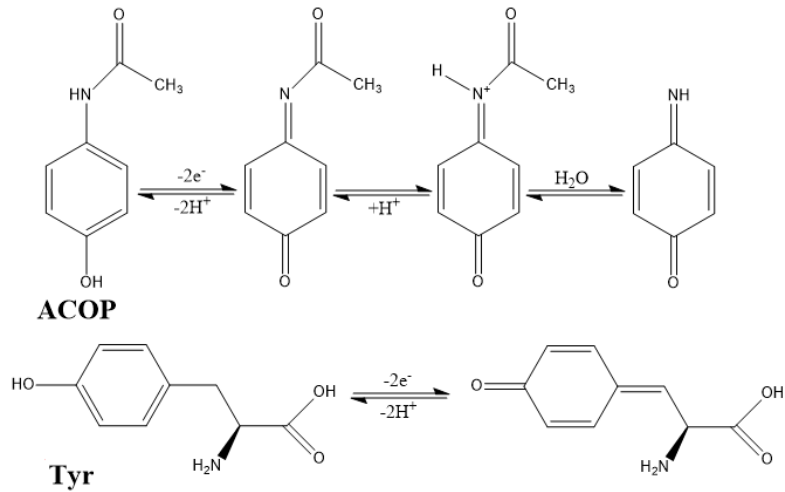


Figure 4. (A) Cyclic voltammetric curves of p-gly/PAA/MWCNTs/SPE in BRBS (a→e: pH 2.0-6.0) containing $10 \mu\text{M}$ of ACOP and $20 \mu\text{M}$ of Try. (B) Corresponding cyclic voltammetric peak current analysis of ACOP and Try in BRBS (pH 2.0-6.0). (C) Corresponding cyclic voltammetric peak potential analysis of ACOP and Try in BRBS (pH 2.0-6.0).



Scheme 1. Probable oxidation mechanism for ACOP and Tyr.

3.3. Analytical performance of the sensor

3.3.1 Calibration curve and detection limit

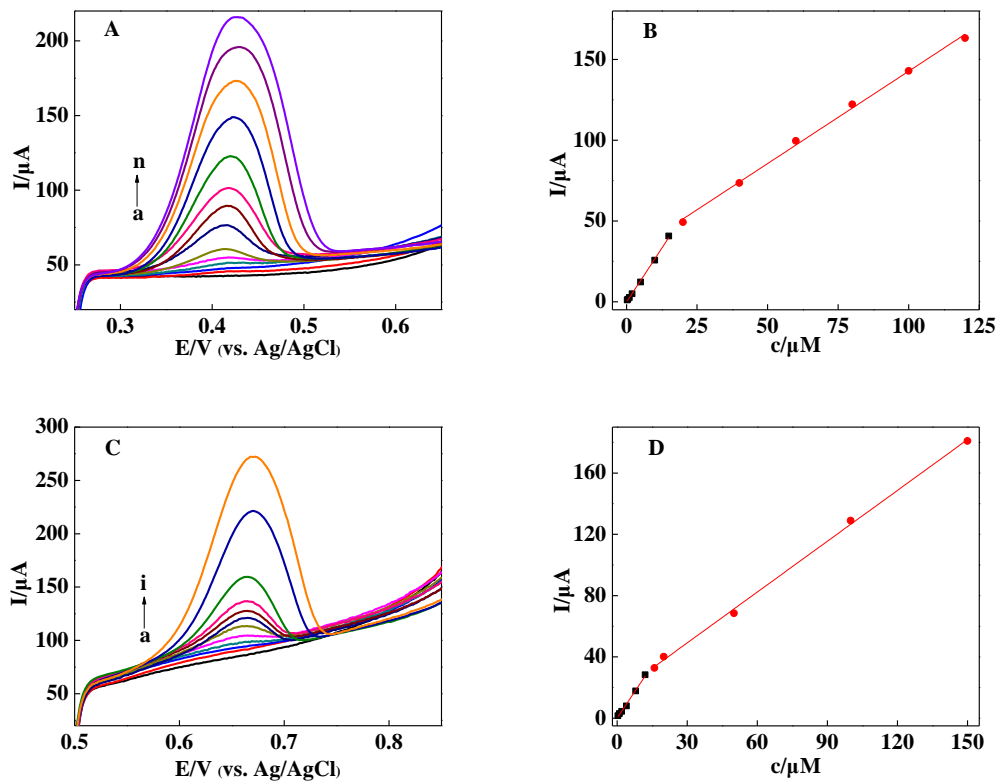


Figure 5. (A) LSV responses from successive additions of ACOP in BRBS (pH 2.0) at p-gly/PAA/MWCNTs/SPE. (B) Typical calibration plots corresponding to ACOP additions up to 120 μM . (C) LSV responses from successive additions of Tyr in BRBS (pH 2.0) at p-gly/PAA/MWCNTs/SPE. (D) Typical calibration plots corresponding to Tyr additions up to 150 μM . Scan rate: $50 \text{ mV} \cdot \text{s}^{-1}$.

As shown in Fig. 5A and Fig. 5B, the LSV analysis was performed in the different concentrations of ACOP at p-gly/PAA/MWCNTs/SPE in BRBS (pH 2.0). The LSV response of ACOP increased with the increase of concentration. And the calibration curves of ACOP showed two linear parts, which intersected at 18.5 μM (0.25-18.5 μM : $I_{pa} (\mu\text{A}) = 2.667c (\mu\text{M}) - 0.213$, $R^2 = 0.997$; 18.5-120 μM : $I_{pa} (\mu\text{A}) = 1.144c (\mu\text{M}) + 28.351$, $R^2 = 0.997$). The detection limit of ACOP was obtained as 0.08 μM . The Fig. 5C and Fig. 5D showed the LSV analysis, which was performed in the different concentrations of Tyr at p-gly/PAA/MWCNTs/SPE in BRBS (pH 2.0). The oxidation peak current increases linearly with the increase of Tyr concentration. And the calibration curves of Tyr showed two linear parts, which intersected at 13.5 μM (0.4-13.5 μM : $I_{pa} (\mu\text{A}) = 2.288c (\mu\text{M}) + 0.064$, $R^2 = 0.994$; 13.5-150 μM : $I_{pa} (\mu\text{A}) = 1.108c (\mu\text{M}) + 15.932$, $R^2 = 0.998$). The detection limit for Tyr was obtained as 0.13 μM . The two linear parts in the ACOP/Tyr calibration curve may be due to the effect of the target molecule concentration on the adsorption between the target molecule and the sensing interface. The probability of contact between single target molecule and sensing interface decreased when the concentration of target molecule was high. This phenomenon is consistent with other relevant literatures, such as references [2] and [22].

3.3.2 Simultaneous determination of ACOP and Tyr

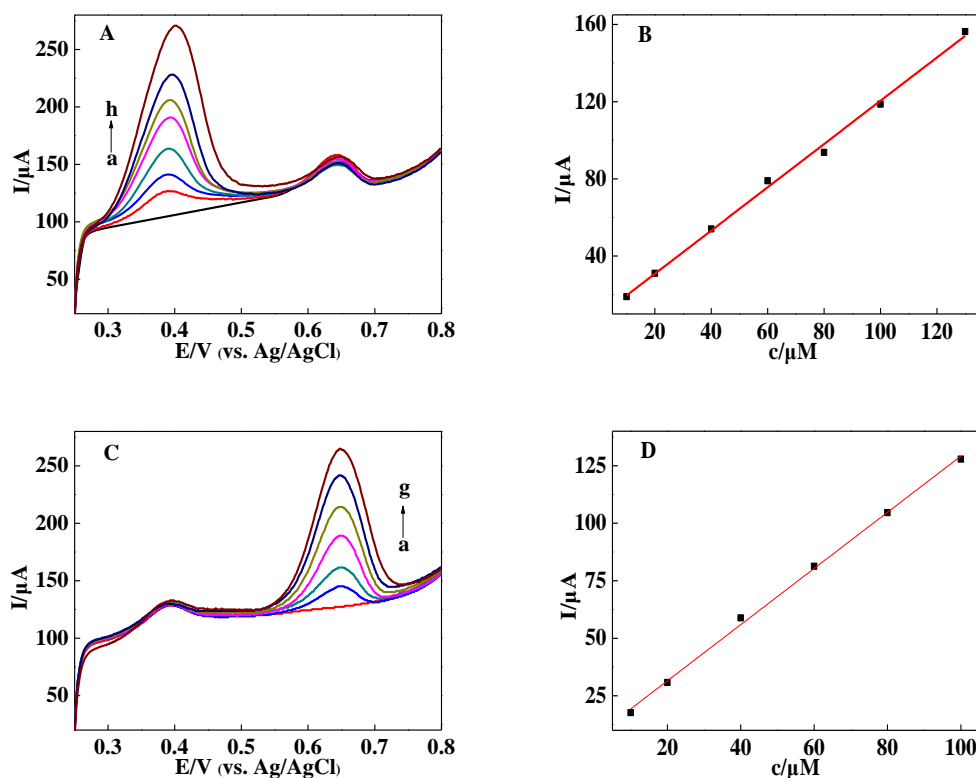


Figure 6. (A) LSV curves of successive addition of ACOP in presence of 10 μM Tyr and (B) Corresponding peak current as function of ACOP concentrations. (C) LSV curves of successive addition of Tyr in presence of 10 μM ACOP and (D) Corresponding peak current as function of Tyr concentration. Scan rate: $50 \text{ mV} \cdot \text{s}^{-1}$.

In order to further study the interaction between ACOP and Tyr, LSV experiments for simultaneous determination of ACOP and Tyr were carried out in BRBS (pH 2.0). As shown in Fig. 6A, when ACOP content increased from 10 $\mu\text{mol}\cdot\text{L}^{-1}$ to 130 $\mu\text{mol}\cdot\text{L}^{-1}$ in presence of 10 μM Tyr, LSV curves revealed that two well-separated and distinct oxidation peaks of ACOP and Tyr were observed. With the continuous addition of ACOP, there was no significant change in Tyr's response. The calibration curve of ACOP was shown in Fig. 6B ($I_{pa} (\mu\text{A}) = 1.121c (\mu\text{M}) + 8.340$, $R^2 = 0.997$). LSV curves of successive additions of Tyr were shown in Fig. 6C, the concentration of ACOP was maintained at 10 $\mu\text{mol}\cdot\text{L}^{-1}$. The LSV response of ACOP also did not change significantly with successive addition of Tyr. A linear relationship for Tyr from 15 to 100 μM was presented in Fig. 6D ($I_{pa} (\mu\text{A}) = 1.220c (\mu\text{M}) + 7.132$, $R^2 = 0.998$). These results indicated that Tyr/ACOP can achieve good detection in presence of ACOP/Tyr.

3.4. Repeatability and stability of p-gly/PAA/MWCNTs/SPE for ACOP and Tyr determination

Repeatability and stability are very important for a sensor. In order to verify the repeatability and stability of the p-gly/PAA/MWCNTs/SPE, LSV responses of five individual sensors towards ACOP and Tyr determination in a solution containing 10 μM ACOP and 20 μM Tyr were recorded every 2 days during 10 days, respectively. After 10 days, LSV response of ACOP/Tyr retained over 91.8% of its initial response. Comparison of five individual sensors, the satisfied relative standard deviation (RSD) for ACOP was less than or equal to 3.7%, while the RSD for Tyr was less than or equal to 4.1%. The results confirmed that electrochemical responses of the proposed sensors towards ACOP and Tyr determination were stable and repeatable.

3.5 Comparison of proposed method with literature methods

Table 1. Comparison with other modified electrode for determination of ACOP and Tyr.

Electrode	Target molecule	Linear range (μM)	LOD (μM)	Ref.
AuNPs/MWCNTs/GCE	Tyr	0.4-80	0.2	[8]
AuNPs/poly (trisamine)/GCE	Tyr	3.9-61.8	0.9	[25]
AuNPs/PTAT/GCE	Tyr	10-560	2	[26]
PbO ₂ /CCE	Tyr	5-1458	0.77	[27]
MWCNTs-GNS/GCE	Tyr	0.9-95	0.19	[28]
Nevirapine/CPE	ACOP	2-12	0.77	[29]
(CMWCNTs-NHCH ₂ CH ₂ NH) ₆ /GCE	ACOP	1-200	0.092	[30]
Boron-doped Diamond Electrode	ACOP	2.99-283	0.768	[31]
Chitosan/CPE	ACOP	0.8-200	0.508	[32]
C-Co ₃ O ₄ /FTO	ACOP	10-6000	1.18	[33]
NiO/CNTs/DPID/CPEs	ACOP	0.8-550	0.3	[34]
CoTPyPRu(bipy) ₂ -Ba /GCE	Tyr	5-750	1.0	[35]
	ACOP	1-50	0.1	
EFTAG/CPE	Tyr	1-24	0.5	[36]
	ACOP	1-150	0.5	
p-Gly/PAA/MWCNTs/SPE	ACOP	0.25-18.5	0.08	This work
		18.5-120		
	Tyr	0.4-13.5	0.13	
		13.5-150		

In Table 1, the results obtained by this modified electrode have been compared with previously reported modified electrodes. It was found that p-gly/PAA/MWCNTs/SPE shows favorable analytical performance in terms of wide linear range and low detection limit over other electrodes. Therefore, the proposed p-gly/PAA/MWCNTs/SPE could be effectively used for the determination of ACOP and Tyr.

3.6. Determination of ACOP and Tyr in real samples

In order to evaluate the potential utility of the fabricated sensor, the p-gly/PAA/MWCNTs/SPE was further applied to detect ACOP and Tyr in human serum samples. As shown in Table 2, the quantitative recoveries for ACOP and Tyr were 95.8% to 100.5% ($RDS \leq 2.7$) and 104.3% to 105.8% ($RDS \leq 3.3$), respectively. These results demonstrated that the developed sensor possesses excellent accuracy and reliability for determination of ACOP and Tyr in real samples.

Table 2. Analytical results for Tyr in human serum samples (n=5).

Added/(μM)		Determined/(μM)		Recovery/%		RSD/%	
ACOP	Tyr	ACOP	Tyr	ACOP	Tyr	ACOP	Tyr
0	0	-	1.37	-	-	-	-
15	25	14.37	26.21	95.8	104.8	2.7	3.1
25	15	25.07	15.87	100.3	105.8	2.1	3.3
25	25	25.12	26.07	100.5	104.3	2.2	2.9

4. CONCLUSION

In this work, we have demonstrated the fabrication of a screen-printed electrochemical sensor based on MWCNTs-doped p-gly/PAA conducting polymers for the simultaneous determination of ACOP and Tyr. The proposed electrochemical sensor demonstrated high selectivity, sensitivity and stability for the determination of ACOP and Tyr at low concentrations. Furthermore, the sensor was used for the determination of ACOP and Tyr in human serum samples. The proposed methods are expected to become an effective tool for the simultaneous determination of ACOP and Tyr in real samples.

References

1. A. Bertolini, A. Ferrari, A. Ottani, S. Guerzoni, R. Tacchi and S. Leone, *CNS drug reviews*, 12(2006)250-275.
2. B. G. Mahmoud, M. Khairy, F. A. Rashwan and C. E. Banks, *Anal. Chem.*, 89(2017)2170-2178.
3. M. J. Smilkstein, G. L. Knapp, K. W. Kulig and B. H. Rumack, *New Engl. J. Med.*, 319(1988)1557-1562.
4. S. Chitravathi, B. E. K. Swamy, G. P. Mamatha and B. N. Chandrashekar, *J. Mol. Liq.*, 172(2012)130-135.
5. F. L. Weber Jr. and B. J. Reiser, *Digest. Dis. Sci.*, 27(1982)103-110.
6. L. Garcia-Carmona, M. Moreno-Guzman, T. Sierra, M. C. Gonzalez and A. Escarpa, *Sens. Actuat. B-Chem.*, 259(2018)762-767.

7. C. R. Scott, *Am.J.Med. Genet. C*, 142C(2006)121-126.
8. T. Madrakian, E. Haghshenas and A. Afkhami, *Sens. Actuat. B-Chem.*, 193(2014)451-460.
9. L. P. James, P. R. Mayeux and J. A. Hinson, *Drug Metab. Dispos.*, 31(2003)1499-1506.
10. W.Z. Zhang, C. Lang and D. M. Kaye, *Biomed. Chromatog.*, 21(2007)273-278.
11. Sirajuddin, A. R. Khaskheli, A. Shah, M. I. Bhangar, A. Niaz and S. Mahesar, *Spectrochim. Acta A*, 68(2007)747-751.
12. S. Mu, Y. Li, A.G. Tang, L.D. Xiao and Y.P. Ren, *Clin. Chim. Acta*, 413(2012)973-977.
13. S.F. Li, M. Xing, H.Y. Wang, L. Zhang, Y.M. Zhong and L. Chen, *Rsc Adv.*, 5(2015)59286-59291.
14. Y. Huang, X.Y. Jiang, W. Wang, J.P. Duan and G.N. Chen, *Talanta*, 70(2006)1157-1163.
15. M. Arvand and T. M. Gholizadeh, *Colloid Surface B*, 103(2013)84-93.
16. S. A. Kumar, C.F. Tang and S.M. Chen, *Talanta*, 76(2008)997-1005.
17. H. Yang, Z.Q. Wei, S.N. He, T. Li, Y.F. Zhu, L.X. Duan, Y. Li and J.G. Wang, *Int. J. Electrochem. Sci.*, 12 (2017) 11089 - 11101.
18. M. Labib, E. H. Sargent and S. O. Kelley, *Chem. Rev.*, 116(2016)9001-9090.
19. G.X. Wang, A. Morrin, M.R. Li, N.Z. Liu and X.L. Luo, *J.Mater. Chem. B*, 6(2018)4173-4190.
20. F. R. Baptista, S. A. Belhout, S. Giordani and S. J. Quinn, *Chem. Soc. Rev.*, 44(2015)4433-4453.
21. P. Zhou, S. Wang, C.L. Tao, X.K. Guo, L.H. Hao, Q. Shao, L. Liu, Y.P. Wang, W. Chu, B. Wang, S.Z. Luo and Z.H. Guo, *Adv. Polym. Tech.*, 37(2018)2325-2335.
22. Z.Q. Wei, Y.J. Sun, Q.W. Yin, L.X. Wang, S.G. Chen, R. Sheng, D.Y. Pan, H. Yang and S.Q. Li, *Int. J. Electrochem. Sci.*, 13(2018)7478-7488.
23. X.C. Li, Z.G. Chen, Y.W. Zhong, F. Yang, J.B. Pan and Y.J. Liang, *Anal. Chim. Acta*, 710(2012)118-124.
24. H. R. Zare, B. Moradiyan, Z. Shekari and A. Benvidi, *Measurement*, 90(2016)510-518.
25. M. Taei and G. Ramazani, *Colloid Surface B*, 123(2014)23-32.
26. M. Taei, F. Hasanpour, H. Salavati, S. H. Banitaba and F. Kazemi, *Mat. Sci. Eng. C-Mater.*, 59(2016)120-128.
27. H. Heidari and E. Habibi, *J. Iran. Chem. Soc.*, 15(2018)885-892.
28. M. Arvand and T. M. Gholizadeh, *Colloid. Surface. B*, 103 (2013) 84-93.
29. S. B. Tanuja, B. E. K. Swamy and K. V. Pai, *J. Electroanal. Chem.*, 798(2017)17-23.
30. Y.C. Li, S.Q. Feng, S.X. Li, Y.Y. Zhang and Y.M. Zhong, *Sens. Actuat. B-Chem.*, 190(2014)999-1005.
31. A. P. P. Eisele, C. F. Valezi and E. R. Sartori, *Analyst*, 142(2017)3514-3521.
32. Y. El Bouabi, A. Farahi, N. Labjar, S. El Hajjaji, M. Bakasse and M. A. El Mhammedi, *Mat. Sci. Eng. C-Mater.*, 58(2016)70-77.
33. C. W. Kung, C. Y. Lin, R. Vittal and K. C. Ho, *Sens. Actuat. B-Chem.*, 182(2013):429-438.
34. H. Karimi-Maleh, M. R. Ganjali, P. Norouzi and A. Bananezhad, *Mat. Sci. Eng. C-Mater.*, 73(2017)472-477.
35. J. C. Kemmegne-Mbouguen, H. E. Toma, K. Araki, V. R. L. Constantino, E. Ngameni and L. Angnes, *Microchim. Acta*, 183(2016)3243-3253.
36. K. Movlaee, H. Beitollahi, M.R. Ganjali and P. Norouzi, *Microchimica Acta*, 184(2017)3281-3289.